



Dynamics and Impacts of Monsoon-Induced Geological Hazards: A 2022 Flood Study along the Swat River in Pakistan

Nazir Ahmed Bazai^{1,3}, Mehtab Alam^{4,5**}, Peng Cui^{1,2,3*}, Wang Hao¹, Adil Poshad Khan⁵, Muhammad Waseem⁶, Yao Shunyu⁷, Muhammad Ramzan¹, Li Wanhong^{1,3}, Tashfain Ahmed⁸,

¹ Key Laboratory of Mountain Surface Process and Hazards/Institute of Mountain Hazards and Environment, Chinese Academy of Sciences, Chengdu, 610041, China.

² Key Laboratory of Land Surface Pattern and Simulation/Institute of Geographic Sciences and Natural Resources Research, Chinese Academy of Sciences, Beijing 100101, China.

³ China-Pakistan Joint Research Center on Earth Sciences, CAS-HEC, Islamabad 45320, Pakistan.

⁴ Ghulam Ishaq Khan Institute of Engineering Sciences and Technology, Topi 23640, District Swabi, Khyber Pakhtunkhwa, Pakistan.

⁵ Department of Geotechnical Engineering, College of Civil Engineering, Tongji University, Shanghai 200092, China.

⁶ School of Interdisciplinary Engineering & Sciences (SINES), National University of Sciences & Technology (NUST), Sector H-12, Islamabad 44000, Pakistan

⁷ China Institute of Water Resources and Hydropower Research, Beijing 100038, China.

⁸ Deep Tech Lab, Computer Science and Engineering Department, Michigan State University, East Lansing, Michigan 48823, USA.

Correspondence to: Peng Cui [*pengcui@imde.ac.cn](mailto:pengcui@imde.ac.cn) and Mehtab Alam [**mehtab.alam@giki.edu.pk](mailto:mehtab.alam@giki.edu.pk)

Abstract. In response to escalating global climate change and its increasing impacts worldwide, this study investigates the consequences of extreme weather events, focusing on the unprecedented 2022 monsoon season in the Swat River basin of Pakistan. Record-breaking rainfall, exceeding the 1960-2021 averages by 7-8%, triggered catastrophic debris flows and floods, aggravating low-income communities' challenges. The resulting financial instability severely affected millions, causing extensive damage to homes, crops, and transportation. The study employs a multidisciplinary approach, combining field investigations, remote sensing data interpretation, and numerical simulations to identify the factors contributing to debris flow incidents. Analysis of land cover changes reveals a decrease in grasslands and an increase in barren land, indicating the adverse effects of deforestation on the region. Topography and gully morphology are crucial in initiating debris flows, with steep gradients and shallow slope failures predominant. Numerical simulations show that debris flows reached high velocities of 18 m/s and depths of 40 m within 45 minutes. Two debris flows resulted in the formation of dams along the Swat River, intensifying subsequent floods. The study emphasizes the interplay of extreme rainfall and deforestation during the rainy season, rendering the region susceptible to debris flows and hindering restoration efforts. The findings underscore the urgent need for comprehensive disaster mitigation strategies. Recommendations include climate change mitigation, reforestation initiatives, and discouraging construction activities in flood-prone and debris flow-prone regions. The study advocates for enhanced early warning systems and rigorous land use planning to protect the environment and local communities, highlighting the imperative of proactive measures in the face of escalating climate challenges. Additionally, the study investigates the spatial distribution of various events and their consequences, including potential hydro-meteorological triggers, and how such events initiate processes that change mountain landscapes. It also assesses the degree to which the 2022 monsoon can be classified as abnormal. The combination of empirical evidence and practical insights presented in this study highlights research gaps and proposes routes toward attaining a comprehensive comprehension of monsoon-triggered geological hazards and consequences.

Keywords: Climate Change; Geological Hazards; Monsoon Floods; Deforestation, Future Challenges



1. Introduction

Disasters like floods, earthquakes, drought, heat waves, tsunamis, cyclones, etc., devastate the human use system, killing thousands of people and destroying infrastructures worldwide, causing billions of economic losses (O'Brien et al., 2008; Ward et al., 2020). The impact of these disasters fluctuates from country to country depending upon the socioeconomic resilience and geomorphology of the land (Atta-Ur-Rahman, 2010). The registration of economic losses and human casualties due to extreme phenomena is higher in developed countries than in developing countries (Atta-Ur-Rahman, 2010). Developing countries are hot spots for catastrophe events. The CRED (2014) estimation shows that the frequency of disasters increased from 100 disasters per decade from 1900 to 1940, whereas 2080 disasters were extreme from 1900 to 2000.

In 2013, Asia was the third hard-hit region, with approximately 88% of casualties from all kinds of disasters compared to an average of 62% decadal. In the same year, Pakistan was classified as fifth-ranked among the most affected countries by CRED (2014), whereas German Watched ranked Pakistan as the third among highly affected nations (Kreft et al., 2013). The consequences of global warming are becoming more and more feasible and practical in the form of increasing natural floods and putting people at risk in several ways, mainly in South Asian regions. Compared to China's 16.4% and the US's 21.5% since 1959, Pakistan has released only 0.4% of carbon dioxide, the primary greenhouse gas; however, Pakistan is the worst example to face the most devastating mega-flood each decade.

Climate change has increased the intensity and frequency of hydrometeorology events that are always a significant threat to water, food, energy, infrastructure, and human lives yearly. Temperature changes and highly increased precipitation, especially in the monsoon season, are significant disaster factors in Pakistan (Otto et al., 2023). Monsoons and heavy rainfall are the main factors inducing natural floods and geological hazards (Segoni et al., 2018). The Flush flood and debris flow dominate during heavy rainfall in the mountainous region. The flush flood, characterized by rapid, short-duration, and high-velocity flows, is the primary cause of property damage and casualties (Ma et al., 2020). According to the "NWS Glossary," flash floods are rapid water rises in "a stream or creek above a predetermined flood level, beginning within six hours of the causative event" (Nws, 2009). Flash floods are mainly caused by short-duration and high-intensity rainfalls in watersheds smaller than 260 km² (Davis, 2001; Georgakakos and Hudlow, 1984; Tang et al., 2020). In this article, flash floods include river floods, rainfall-induced landslides, and debris flows. Flash floods are one of the world's most devastating and fatal disasters (Špitalar et al., 2014; Tang et al., 2017).

The flooding in Pakistan and surrounding regions in recent decades has demonstrated its severity and extremes. The most recent and most destructive was the unprecedented monsoon rains in 2022 from June to September triggered one of Pakistan's worst floods in decades, and the Pakistani government declared a state of emergency on August 25th, according to Pakistan's National Disaster Management Authority (NDMA). The floods have led to over 1,718 casualties and 12,800 injuries, with the highest fatality rate in Sindh. More than 33 million people (about 15% of the country's total population) were affected by the floods in 84 calamity-declared districts, some 7.9 million people were displaced, and some 598,000 lived in relief camps. Over 287,000 houses have been destroyed, and over 662,000 are partially damaged (NDMA). At the same time, the flood caused damage to roads, railway tracks, telecommunication systems, and other infrastructure to varying degrees, seriously affecting the lives of residents. This disturbance to infrastructure, residences, and livelihoods continues to worsen over time. The situation has been exacerbated by a lack of timely response and identification of climatic factors, inadequate response from residents and local authorities, and the absence of timely implementation of proposed strategies (Shah, 2020).

Recent human-induced changes significantly influence the likelihood of slope movements in how people use the land (Vanacker et al., 2003; Reichenbach et al., 2014) and treat the surroundings of the rivers. Changing from forest land-cover/land-use (LCLU) classes can increase the vulnerability to landslides and intense runoff. Including vegetation enhances slopes' physical stability by augmenting root-soil strength (Hürliemann et al., 2022; Mehtab et al., 2020; Bazai et al., 2021). It reduces erosive forces through the canopy's interception of rainfall drops (Bonnesoeur et al., 2019). Furthermore, slope vegetation has been documented to decrease infiltrating water and lower pore water pressure (Tsukamoto, 1990; Sidle, 1992; Preti et al., 2010). On the contrary, it may also reduce infiltration by encouraging soil crust formation (Bu et al., 2014). Since 1850, the planet has witnessed an alarming and unprecedented destruction of forests, driven mainly by the expansion of industrial capitalism and resulting in a global forest extinction crisis. Forests in the mountainous regions of Pakistan are undergoing rapid degradation, particularly in these areas. The deforestation rate stands at nearly 1.5% (Mehmood et al.,

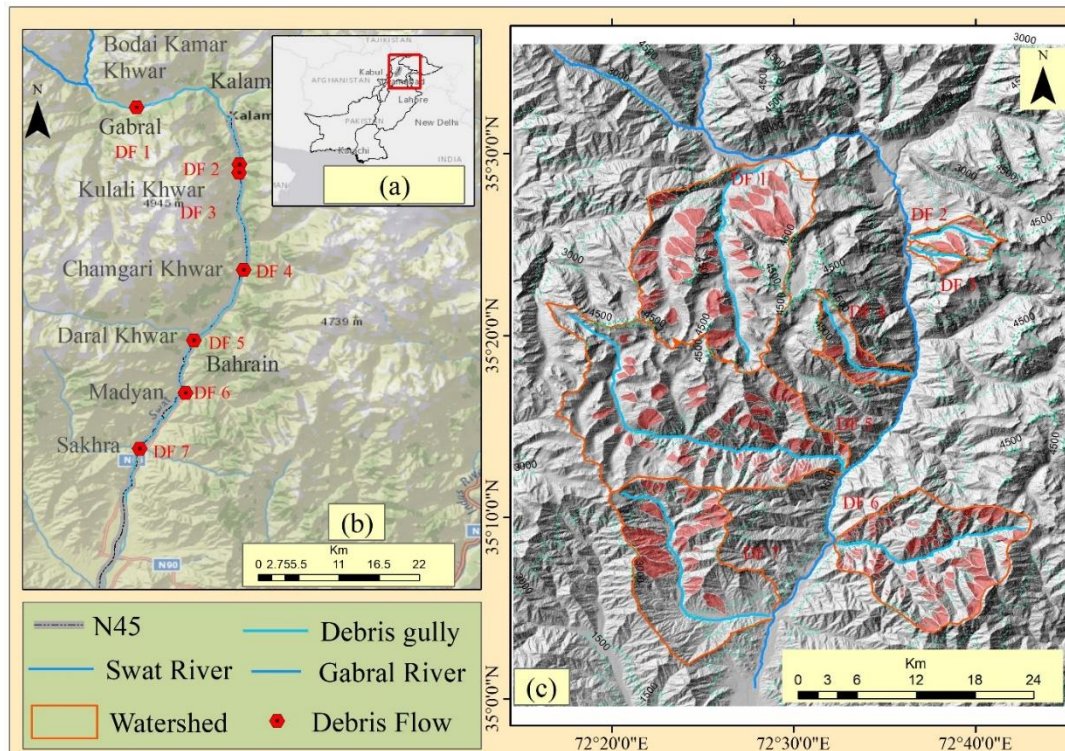


2018), a highly concerning and alarming trend posing a significant threat to the ecosystem, which also often leads to geological hazards and flash flooding in the mountainous region of Pakistan.

95 The different factors contributing to geological hazards have been well identified, but current studies have primarily focused on isolated factors and their potential consequences. However, there remains a gap in research for a comprehensive approach that considers the interplay between extreme climate events and geological hazards, incorporating various triggering factors, the intensity of debris flow, and their resulting consequences. To address this research gap, this paper has explored the geological, physical, and dynamic attributes of debris flows, the consequences of debris flows leading to floods and infrastructural damages, and the role of human activities in increasing vulnerability and the risk of economic and life
100 losses. It then delves into the correlation between debris flow occurrence conditions and associated rainfall, offering insights into hazard prediction and warning systems. Furthermore, the impact of deforestation on the initiation of debris flow was investigated through field and numerical studies. Lastly, it presents recommendations for mitigation strategies, guiding government authorities in preventing future debris flow hazards.

2. Study Area

105 The district Swat is located in northern Pakistan (Fig. 1), a natural geographic region surrounding River Swat. River Swat is nourished all year round by glacier streams from its source in the Hindu Kush Mountain. At Kalam, where the Usho and Gabral rivers (also known as the Utrar River) converge, the River Swat rises from the high valleys of Swat Kohistan. The River Swat travels from the junction via the Kalam Valley's small gorges until it reaches Madyan. From there, the river flows quietly for 160 km across the lower Swat Valley's plains, ending in Chakdara. The river traverses a small gorge in the southernmost point of the Swat Valley, connecting the Panjkora River near Bosaq before flowing into the Peshawar Valley. Around Charsadda, it eventually comes to an end in the Kabul River. In the extreme southern end of the Swat Valley, the river enters a narrow gorge and joins the Panjkora River at Bosaq before entering the Peshawar Valley. It finally terminates in the Kabul River, near Charsadda.
110





115 **Figure 1.** Location and details of the study area. (a) Study area; (b) Details of the Swat River area and its investigated debris
flow; (c) Catchments of debris flow fans, loose material, and landslides used as the primary source of debris flow. The
source of the background image is © Google Earth.

3. Methodology

120 3.1 Field Investigation

In the last few decades, the northern region of Pakistan, particularly Swat, has experienced a significant history of geological
hazards, especially during the monsoon season. As a result of these occurrences, roads often become impassable due to
various geological hazards such as landslides and debris flows (Islam et al., 2022b). In the monsoon season of 2022, heavy
rainfall led to several landslides and debris flows, causing casualties that were extensively covered by the media. After
125 consulting different local government bodies of Pakistan, i.e., the Communication and Works Department and Provisional
Disaster Management Authorities (PDMA), the various locations of catastrophic geological hazards were identified through
extensive field visits. The sites were then physically visited to study the root cause of the identified geological risks. The
predominant geological hazards observed in the area were landslides and debris flows (DF). The authors carefully
documented the location of each landslide and debris flow using GPS, with an accuracy of 1m. They also utilized measuring
130 tape to determine the dimensions of these landslides. Furthermore, the positions of each debris flow dam and meticulously
measured the dimensions of each debris flow for their comprehensive documentation. The data collected from the field visits
were then analyzed to understand the features of the debris flow source areas, the flow paths, and flow deposits in the study
region. The gully of each identified debris flow was surveyed on the ground, and understanding was gained about defining
the source conditions and the characteristics of the flow channel and the depositional fan. The identified geological hazards
135 were mapped using a basic geographical information system (GIS). After an extensive survey of the debris flow gully, the
damage assessment of structures in the study area was conducted. The debris flows were categorized into different
intensities, namely low, medium, high, and very high, based on the extent of damage they caused and the volume of debris
involved.

3.2 Metrological data

140 Rainfall records from the meteorological station near Kalam Swat (Lat = 35°50', Long. = 72°59') were used to determine the
daily rainfall totals during all the debris flow events. Hourly precipitation data collected at the rain gauge station were used
to determine the rainfall intensity/duration for each debris flow-producing rainstorm. The precipitation data were collected
from the Meteorological Department of Pakistan (PMD). On August 26, 2022, the Irrigation Department of Khyber
Pakhtunkhwa (KPK) reported a record-breaking flood discharge of 227,899 cusecs from the River Swat, creating a
145 hazardous situation for the residents in its vicinity.

3.3 land use and land cover (LUC)

Various types of land use and land cover (LUC) can impact the stability of slopes due to their ability to alter the hydrological
processes of hillslopes, the distribution of rainfall, the characteristics of infiltration, runoff generation, and even the shear
strength of the soil itself (García-Ruiz et al., 2010). However, unlike numerous environmental factors like geological
150 structure and lithology, land use and land cover (LUC) have the potential to undergo seasonal or rapid changes due to the
combined effects of natural processes and human activities (Reichenbach et al., 2014)). Therefore, in regions characterized
by rapid fluctuations in land use and land cover (LUC) within a short timeframe, it becomes crucial to investigate the
influence of LUC on landslides (Ali et al., 2012). A comparative analysis spanning at least two distinct periods is necessary
for LUC mapping to capture the LUC changes, as Pisano et al. (2017) outlined. The present study examined 20 years (2002–
155 2022), segmented into 04 intervals: 2002, 2009, 2016, and 2022. The analysis utilized MODIS MCD12Q1 V6.1 data
obtained from the USGS Earth Explorer platform (<https://earthexplorer.usgs.gov/>) and involved a comprehensive workflow
executed in ArcGIS. The land cover classification was performed on each year's dataset using ArcGIS tools. This involved
applying appropriate spectral indices, thresholds, and classification algorithms to assign specific land cover categories to
each pixel. Change detection analysis was subsequently conducted by comparing classified maps for consecutive years.
160 Changes in land cover percentages were quantified for each type. Temporal trends in land cover were analyzed by



calculating the percentage distribution of each land cover class across the study period. Emphasis was placed on identifying persistent patterns and notable shifts in vegetation, croplands, barren land, built-up areas, and other land cover types. The results were visualized using thematic maps to illustrate the evolving LULC patterns.

3.4 Governing equations of a numerical method

165 The 2-D debris flow movement model that simplifies the Navier–Stokes equation via the depth-integrated continuum method was adopted to analyze the dynamic processes of the 04 (DF 2, DF 3, DF 4, and Df 5) strong debris flows induced by landslides and loose material by heavy rainfall in the catchments of the study area. The governing equations are as follows:

$$\frac{\partial W}{\partial t} + \frac{\partial F}{\partial x} + \frac{\partial G}{\partial y} = S \quad (1)$$

in which

$$170 \quad W = \begin{bmatrix} h \\ hu \\ hv \end{bmatrix}, F = \begin{bmatrix} hu \\ hu^2 + gh^2 / 2 \\ huv \end{bmatrix}, G = \begin{bmatrix} hu \\ huv \\ hv^2 + gh^2 / 2 \end{bmatrix}, S = \begin{bmatrix} 0 \\ gh(S_{ax} - S_{fx}) \\ gh(S_{ay} - S_{fy}) \end{bmatrix} \quad (2)$$

In this context, h represents the flow height, while u and v denotes the depth-integrated flow velocities in the x and y directions, respectively. The parameter g stands for the acceleration due to gravity, S_{ax} and refers to the momentum source terms in the x and y directions, respectively. Additionally, S_{fx} and S_{fy} are the resistance terms in the x and y directions, respectively. The format of S_{ax} and S_{ay} is as follows:

$$175 \quad S_{ax} = -\frac{\partial Z}{\partial x}, S_{ay} = -\frac{\partial Z}{\partial y} \quad (3)$$

The field investigations revealed that the debris flows were viscous. In debris flow simulations, a viscous debris flow is usually simplified to the Bingham fluid model (Julien and Lan, 1991; Rickenmann et al., 2006; Ying-Hsin et al., 2013). Therefore, the Bingham fluid stress constitutive model was used as the resistance model.

The total Bingham friction S_f is as follows:

$$180 \quad S_f = \frac{\tau_B}{\rho gh} + \frac{K_l \mu_B V}{8 \rho gh^2} + \frac{n^2 V^2}{h^{4/3}} \quad (4)$$

where τ_B is the Bingham yield stress; μ_B is the Bingham viscosity; K_l is the laminar flow resistance coefficient; n is the pseudo-Manning's resistance coefficient; V is the depth-averaged velocity, i.e., $\sqrt{u^2 + v^2}$; and ρ is the fluid density.

The relationship between S_{fx} and S_{fy} , S_f , is as follows:

$$S_{fx} = \frac{u}{\sqrt{u^2 + v^2}} S_f, S_{fy} = \frac{v}{\sqrt{u^2 + v^2}} S_f \quad (5)$$

185 The Massflow software (Ouyang et al., 2013) was used to solve the depth-integrated continuum governing equation. Since the Bingham resistance model is not defined in Massflow, a custom Bingham fluid resistance simulation was performed for the secondary development in Massflow. Experimental benchmarks and simulations of actual events have verified its robustness. It has been widely used in various two-dimensional surface flow simulation cases (Ouyang et al., 2019b; Ouyang et al., 2015a; Ouyang et al., 2015b; Ouyang et al., 2013; Ouyang et al., 2019a; Ouyang et al., 2016).

190

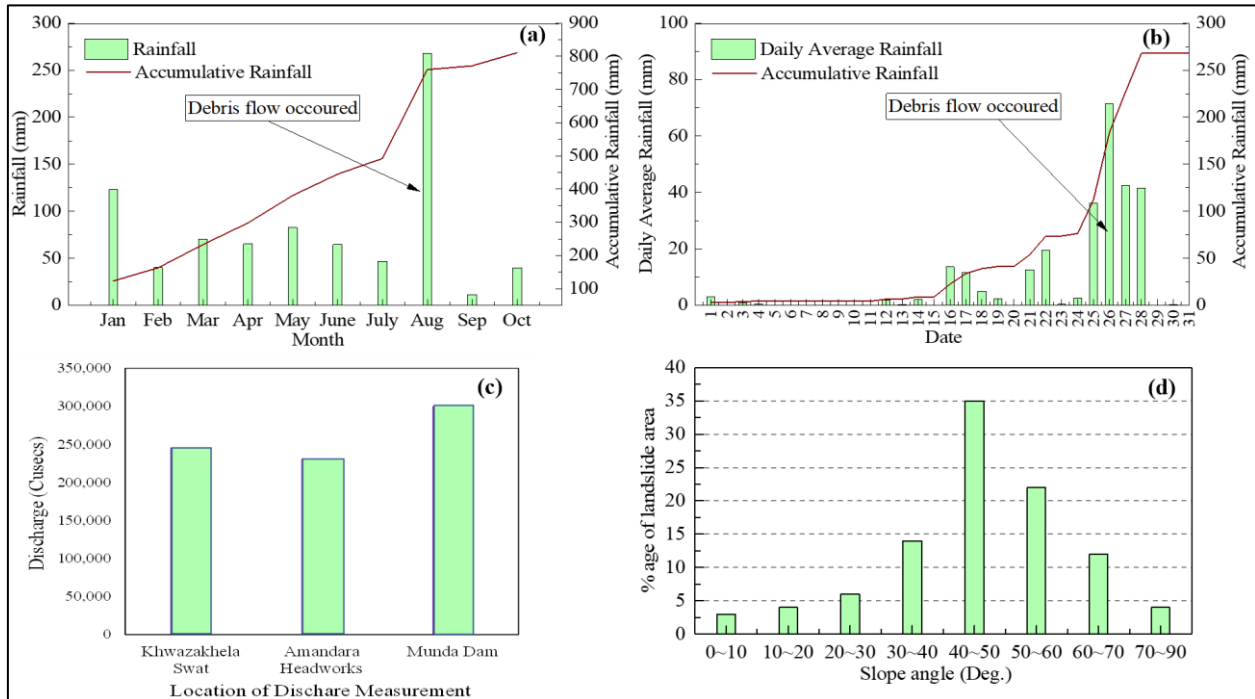


4. Results

4.1. Triggering Rainfall

One of the most crucial initiating elements for landslides and debris flows is rainfall. The relationship between rain and landslides has been established in various places using the characteristics of landslide-triggering rainfall. Cepeda et al. (2010) showed a direct correlation between precipitation thresholds and landslide risk levels. This link provided the foundation for a conceptual approach with susceptibility-based rainfall thresholds. The comparison between pre-deforestation and post-deforestation critical values, which could trigger debris flows, shows that deforestation has modified the conditions.

A rain gauge station at Kalam Valley records hourly data, providing an excellent ground-based rainfall record. This station is located near the debris flow areas with an elevation of 2,000 m. Precipitation generally increases with height in our study area. The average monthly rainfall is shown in Fig. 2a. In contrast, the average daily rainfall for the flood month (August 2022) is given in Fig. 2b. On the 26th of August 2022, heavy rain with an intensity of 71.5 mm/day, coupled with an antecedent rainfall of 40 mm over two days, catalyzed multiple debris flows along the River Swat. These natural events led to a devastating disaster, causing significant damage to various structures in the affected area. The flood discharge reported at different locations is shown in Fig. 2c. The highest discharge at the Munda Dam location was due to flood water from the Panjokar River at Bosaq (the junction points of the Swat River and the Panjkora River upstream of Munda Dam). The return period of the flood is estimated at 425 years. The reported date of flood discharge at Khwazakhela was 22 August 2022, while at Amandara Headworks (Batkhela) and Munda Dam (Mohmand Agency), it was 26 August 2022.



210 **Figure 2.** Precipitation data for the meteorological station at Kalam for the year 2022 (a & b), Precipitation data for the meteorological station at Kalam for August 2022 (c), Discharge measured at different locations along the Swat River during Flood 2022 (d), Landslide density in an area with varying angles of slope



4.2. Flood Level at different locations

215 The flood levels at various points along the Swat River and its tributaries are summarized in Table 01. In places where the riverbanks are constrained by buildings, like Kalam, Bahrain, and Madyan, flood levels reached 50 to 80 ft. Conversely, more comprehensive river sections with no residential encroachments, such as Chakdara and Batkhela, experienced 35 to 50-foot flood levels. The most extreme and high-magnitude floods occurred at Bodai Kamar Khwar, reaching 70 to 80 ft. Notably, the junction of Swat and Panjkora Rivers surged to 95 to 105 ft, significantly contributing to residential inundation.

Table 1. Flood Level observed at different locations along the Swat River during Flood 2022

| Location | Flood Level (ft) |
|-------------------------------------------------------|------------------|
| Gabriel (Starting point of Swat River) | 40 |
| Kalam | 50-60 |
| Bahrain | 70-80 |
| Madyan | 70-75 |
| Khwazakhela | 45-50 |
| Chakdara (at Chakdara Bridge) | 30 |
| Batkhela (at Amandara Headworks) | 25 |
| Malakand Agency | 50 |
| Bosaq (<i>Junction of Swat and Panjkora Rivers</i>) | 95 -105 |
| Munda dam | 70 |
| Dagai (District Charsada) | 40-45 |
| Nowshera (<i>Kabul River</i>) | 25-30 |
| Flood Level in Swat Tributaries | |
| Bodai Kamar Khwar | 50 |
| Changari Khwar | 60 |
| Bodai Kamar Khwar | 70-80 |
| Daral Khwar | 40 |

220

4.3. Debris flow occurrence influenced by topographic factors

225 The correlation between the volume of debris materials contributed by landslides and the total magnitude of debris flow events strongly depends on the topography of the gully. Typically, areas with steeper slopes and more significant elevations exhibit increased vulnerability to landslide and debris flow occurrences. Based on the data extracted from the 25-m digital elevation model, it was observed that debris flows predominantly originated from steep slopes within relatively small drainage gulleys. The data presented in Table 2 indicates that the average slope angles within the debris flow initiation zones ranged from 30° to 45°. The data depicted in Fig. 2d reveals that 87% of the landslides triggered by rainfall occurred in areas with slope angles exceeding 30°, whereas 83% occurred within the range of slope angles between 40° and 70°. The significance of slope steepness cannot be overstated when it comes to influencing the incidence of debris flows. This is primarily because most debris flows are initiated as shallow landslides or from eroded rills or gullies on substantial landslide deposits. In general, it can be concluded that debris flows are prone to be triggered on slope angles exceeding 30°.

230

4.4. Land Use and Land Cover

235 The most prominent observation is the consistent and alarming decline in vegetation cover across various components. Grassland, a critical biome, substantially decreased from 42% in 2001 to 35% in 2022 (Fig. 03). broadleaf forest cover dwindled from 12% to 8% during the same period. Other vegetation categories also demonstrated declining trends, signifying a pervasive and persistent loss of vegetative landscapes. In contrast, the cropland category displayed fluctuations, potentially indicating changing agricultural practices or land management strategies. Barren land witnessed a notable



240

expansion, escalating from 15% in 2001 to 24% in 2022. This transformation highlights increased land degradation and shifts in land utilization. The built-up areas category displayed a parallel increase, emphasizing urbanization's encroachment on natural habitats. Water bodies and snow cover exhibited relatively minor fluctuations, indicating relative stability in these categories. The findings underscore the urgency of addressing the ongoing vegetation loss and increasing barren land through targeted conservation efforts, sustainable land management, and informed policy decisions.

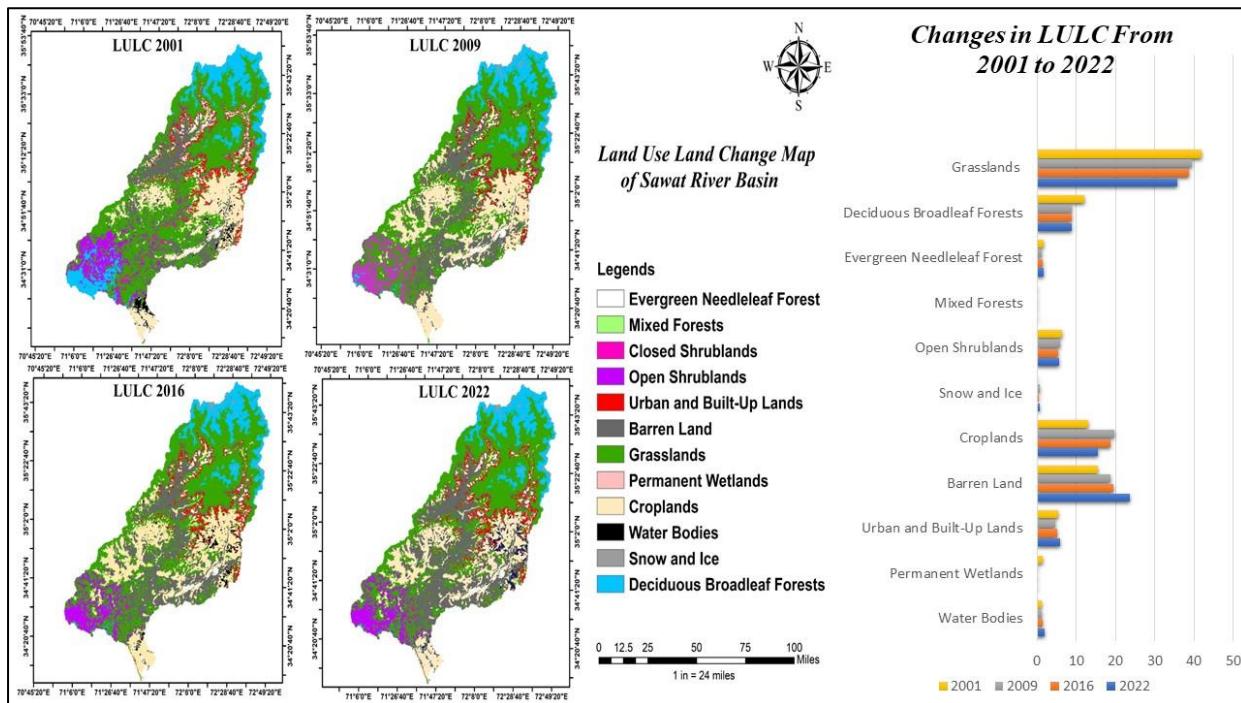


Figure 3. Land Use Cover Change in the Swat River Basin (2001-2022) divided into four intervals. Visualized maps are displayed on the left, while the corresponding temporal trend is presented in the right-hand panel.

245

4.5. Debris Flow fans

The extensive rainfall from August 22, 2022, to August 28, 2023, has triggered numerous debris flows in the Swat area. These debris flows accumulated debris, mud, and rock on the national highway N – 95 (Fig. 1) along the river Swat. Debris flows stand out as one of the most challenging natural events that can happen in mountainous areas, as recognized by Alexander (1991) and Hürlimann et al. (2006). Because the most significant destruction often occurs where debris flows come to rest, it is crucial to carry out detailed hazard assessments for these fan areas. This helps protect people and buildings from future debris flows and allows us to manage the associated risks better (Prochaska et al., 2008). In the surveyed region, we found 07 gullies adjacent to the River Swat that experienced debris flows during the heavy rainfall incident, as shown in Figure 4 (a). The majority of the debris flow made its way to the River Swat. These alluvial fans formed debris dams that entirely or partially obstructed the River Swat at its confluence with its tributaries. Consequently, the breakage of these unconsolidated dams resulted in widespread flooding along the River Swat. Roads, bridges, and houses suffered significant destruction due to the debris flows. The 07 debris flow catchment areas surveyed were analyzed for their morphological characteristics, summarized in Table 2 and Fig. 4. The catchment areas have a surface area ranging from 7.1 to 155 km². The

255

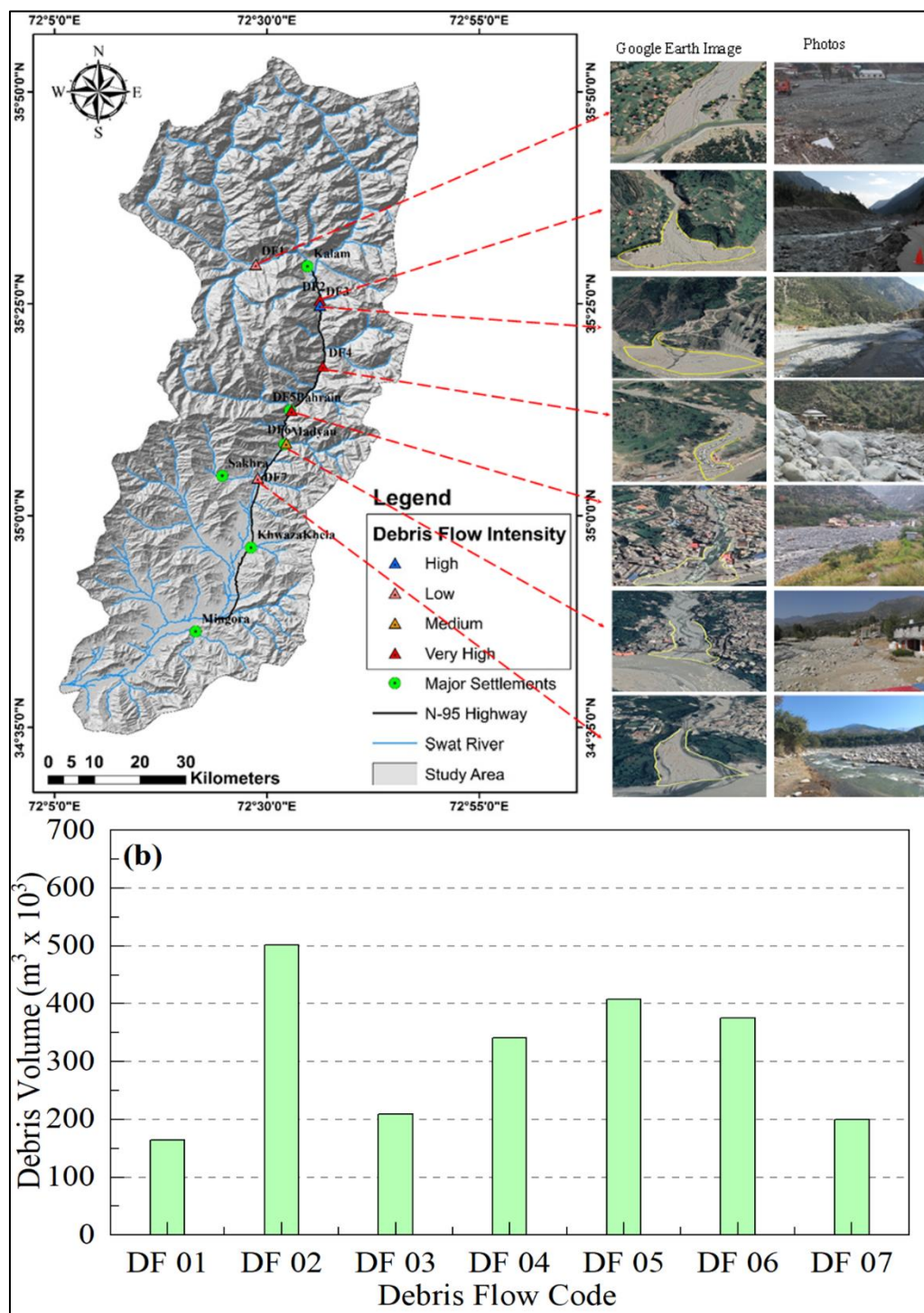


260 identified debris flow channels were long and steep (length 5 km; average channel gradient, $>30^\circ$). The catchment source areas have an internal relief that varies from 1.5 to 3 km, as shown in Table 2.

Table 2: Morphological characteristics of the 07 debris flow

| Gully Code | Gully Name | Basin Area Km ² | Channel Length (Km) | Min Elevation (m) | Max Elev (m) | Basin Relief (m) | Channel Gradient | The slope of Initiation Zones (Degrees) | Avg Slope | Whether Debris flow has an accumulation fan (yes, no) | The shape of the accumulation fan |
|------------|------------------------------------------|----------------------------|---------------------|-------------------|--------------|------------------|------------------|-----------------------------------------|-----------|-------------------------------------------------------|---------------------------------------|
| DF 1 | Gabral | 224 | 26 | 2222 | 4399 | 2177 | 32 | 77.8 | 10 | Yes | biased downstream |
| DF 2 | Bodai Kamar Khwar (Bahrain – Kalam Road) | 18.9 | 8.66 | 1900 | 4992 | 3092 | 40 | 77.1 | 32.1 | Yes | The river erodes symmetrical and toe. |
| DF 3 | Kulali Khwar (Bahrain Kalam Road) | 7.1 | 5.16 | 2886 | 4418 | 1532 | 41 | 87 | 41.1 | yes | completely eroded |
| DF 4 | Chamgari Khwar (Bahrain – Kalam Road) | 26.7 | 13.5 | 3081 | 4629 | 1548 | 35 | 70.3 | 23.1 | yes | completely eroded |
| DF 5 | Daral Khwar (Bahrain) | 277 | 33.4 | 2625 | 4370 | 1745 | 33 | 77.6 | 12 | Yes | biased downstream |
| DF 6 | Madyan | 143 | 18.6 | 2122 | 4062 | 1940 | 41 | 73.3 | 17.7 | yes | biased downstream |
| DF 7 | Sakhra (Khazakhela) | 155 | 24.8 | 1972 | 3795 | 1823 | 38 | 53.9 | 11.1 | yes | biased downstream |

265 We conducted a rapid field measurement using handheld GPS devices and laser rangefinders to estimate the volume of the debris flow fans and the boundaries of the debris flow were established using the survey data points. The volume of debris flow estimates is shown in Fig. 4b. The debris fan volume for the smallest one was $164.063 \times 10^3 \text{ m}^3$, and the volume for the largest one was $501.363 \times 10^3 \text{ m}^3$, while the mean volume estimated was $291.658 \times 10^3 \text{ m}^3$. We evaluated the sizes of the deposits on the fans using the techniques recommended by Stoffel (2010).

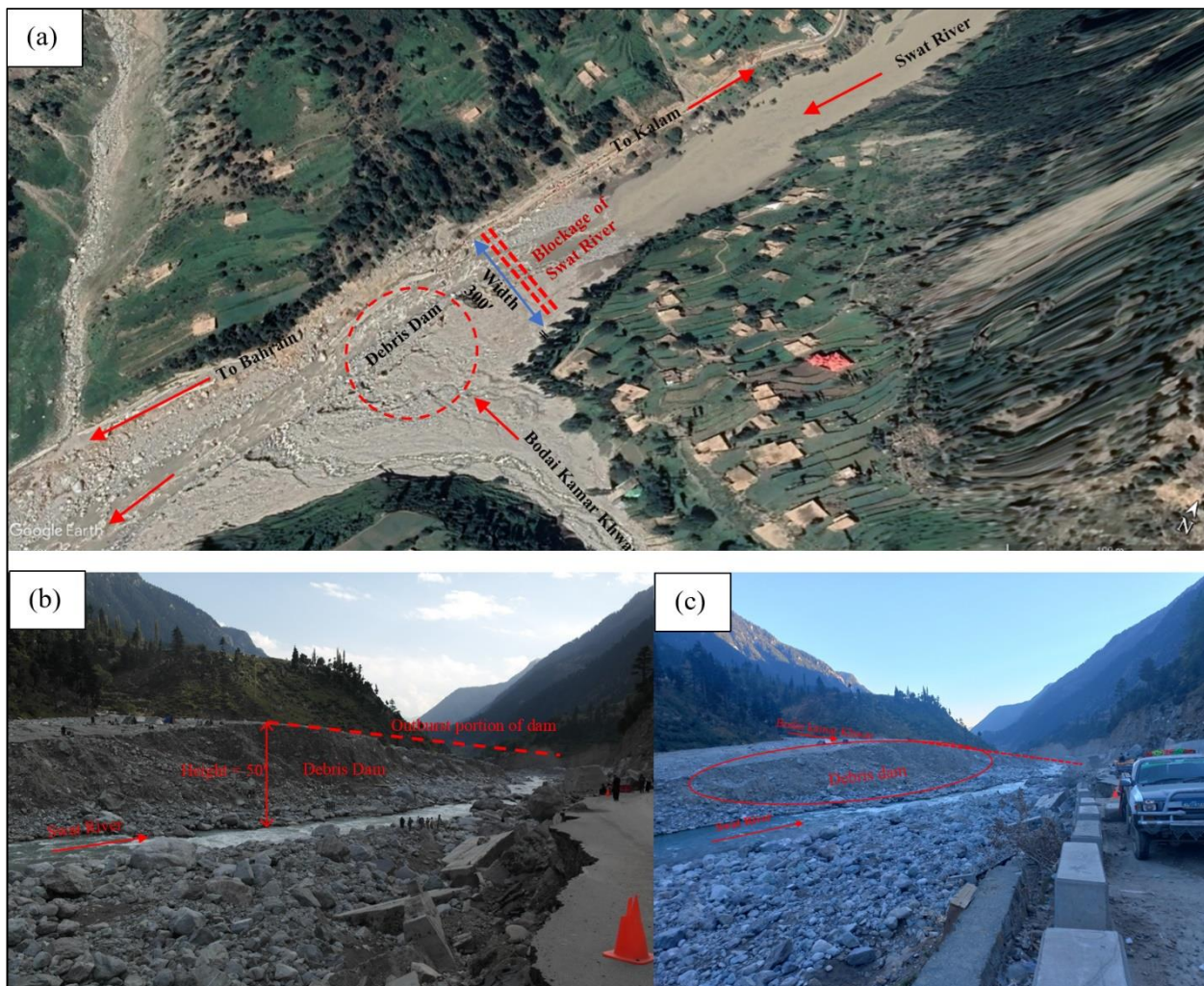


270 **Figure 4.** (a) Geographic location, catchments, and intensity of debris flows (DF1 to 7) gullies in the Swat River basin. Debris flow intensity is categorized from low to very high. (b) Accumulated debris fan volume. The background image is a source of © Google Earth and field visit.



4.6. The triggering reason and sources for the Debris flow

275 Analysis of aerial photographs and on-site field surveys revealed severe ground erosion due to intense monsoon rainfall on steep terrain. Individual landslides or erosion are responsible for baring the mountains (Figs. 5-7). Most landslides began as relatively thin earth slides or debris slides, comprising soil mixed with rock fragments, gaining momentum as they absorbed more water and transformed into debris flows. Another way landslides began was through the formation of small channels, known as rills, on the landslide deposits. These rills gradually deepened downstream due to erosion. When these rills formed on the landslide deposits, they funneled surface water runoff and caused it to flow in a more defined path. Consequently, this
280 concentrated flow led to the mobilization and transportation of substantial sediment into the drainage network, resulting in the scouring of the channels (Fig. 6).



285 **Figure 5.** Details of the debris dam created by debris flow in Bodai Kamar gully (DF 2) (a) Aerial view of the debris dam (b) Frontal perspective post-failure, illustrating the height and outburst section of the debris dam (c) Panoramic view of the



debris dam after failure. The background image for panel (a) is taken from © Google Earth and the other panels during the field visit.

290 Among the identified debris flows, DF 2 and DF 5 (Fig. 4a) were catastrophic. DF 2 originated from Budai Kamar (lat= 35°25'26.48", Long = 72°36'14.25") valley and managed to traverse the River Swat, creating a natural debris dam. This dam was approximately 50 feet in height, 500 feet long across the river, and 300 feet wide along the river section (Fig. 5). The dam blocked the River Swat for 27 hours. The breakage of the natural dam increased the discharge in the River Swat downstream of Kalam Valley, resulting in a considerable flash flow with debris in the River Swat. The stream's debris flow was due to erosion of the stream sides, causing shallow landslides (Fig. 6) along the stream's path, leading the debris to flow with the flash flood. The general height of landslides in the stream ranged from 25 ft to 100 ft (Fig. 6). The Budai Kamar Valley (DF 2) is located on the left bank of River Swat and has a catchment area of 18.9 km² and a channel length of 8.66 km (Table 2). The catchment area of Budai Kamar Valley was determined using a 25-m DEM and on-site photos taken on 30 August 2022.





300 **Figure 6.** Through field investigation, identified Source areas, stream erosion, and landslide deposits contributing to debris
flow events at Bodai Kamar (DF 2) locations throughout the event. The background image for Bodai Kamar Khwar is taken
from © Google Earth and the other panels during the field visit.

305 The DF 5 originated in the Daral valley near Bahrain Bazar (Fig. 7). The Daral stream joins the River Swat near
Bahrain Bazar. The extensive debris in the Daral Khwar blocked River Swat and diverted flows to Bahrain Bazar, which led
to devastating damage to structures. The catchment area of the Daral Khwar is 277 km² and has a chanal length of 33.4 km.
The stream's debris flow was due to erosion of the stream sides, which caused shallow landslides (Fig. 6) along the stream's
path, leading the debris to flow with the flash flood. The general height of landslides in the stream ranged from 30 ft to 70 ft



(Fig 7)

310 **Figure 7.** Through field investigation, identified Source areas, stream erosion, and landslide deposits contributing to debris
flow events at the Daral Khwar (DF 5) location throughout the event. The background image for Daral Khwar is taken from
© Google Earth and the other panels during the field visit.



315 Based on our field observations of the debris flows, they appear to be triggered by substantial sheetwash and rill erosion. The intense rainfall upstream of the channel was pivotal in setting these processes in motion. As the flows advanced through the lowest parts of the gully's channel, their volume increased due to the accumulation of runoff and additional eroded material from the adjacent slopes, tributary channels, and even shallow landslides on the hillsides. Moreover, the flows also swept up larger sediment pieces stored within the channel, eventually making their way out of the catchment mouths. These more prominent elements were embedded within a finely-grained matrix, creating a mix of boulder-sized material abundant in the debris.

4.7. Simulated Debris flow depth and velocity

320 The flow depth (Fig. 8 a-e) and velocity (Fig.8 f-j) of debris flow movements triggered in four catchments (DF 2, DF 3, DF 4, and DF 5) were illustrated. The analysis covers specific time intervals: $t = 0$ min, 15 min, 30 min, 45 min, and 60 min. The initial conditions of the debris flow, originating from the source zone at $t = 0$ min before the activation of velocity from the source areas, are depicted in Fig. 8a and f. As the movements progress, at $t = 15$ min, the flow velocity gradually increases, reaching 8 m/s (Fig. 8 g) in the Daral Khwar streams (DB 5). Simultaneously, the flow depth at the same time is recorded as 10 to 20 m (Fig. 8 b) in the Swat River. Due to the Daral Khwar debris flow merging with the Swat River, the depth of the debris flow in the stream reaches 20-29 m. The depth and velocity increase rapidly with the advancement of the bulbous front, as Iverson et al. (2010) observed because all debris flow streams merge almost simultaneously with the Swat

325



River.

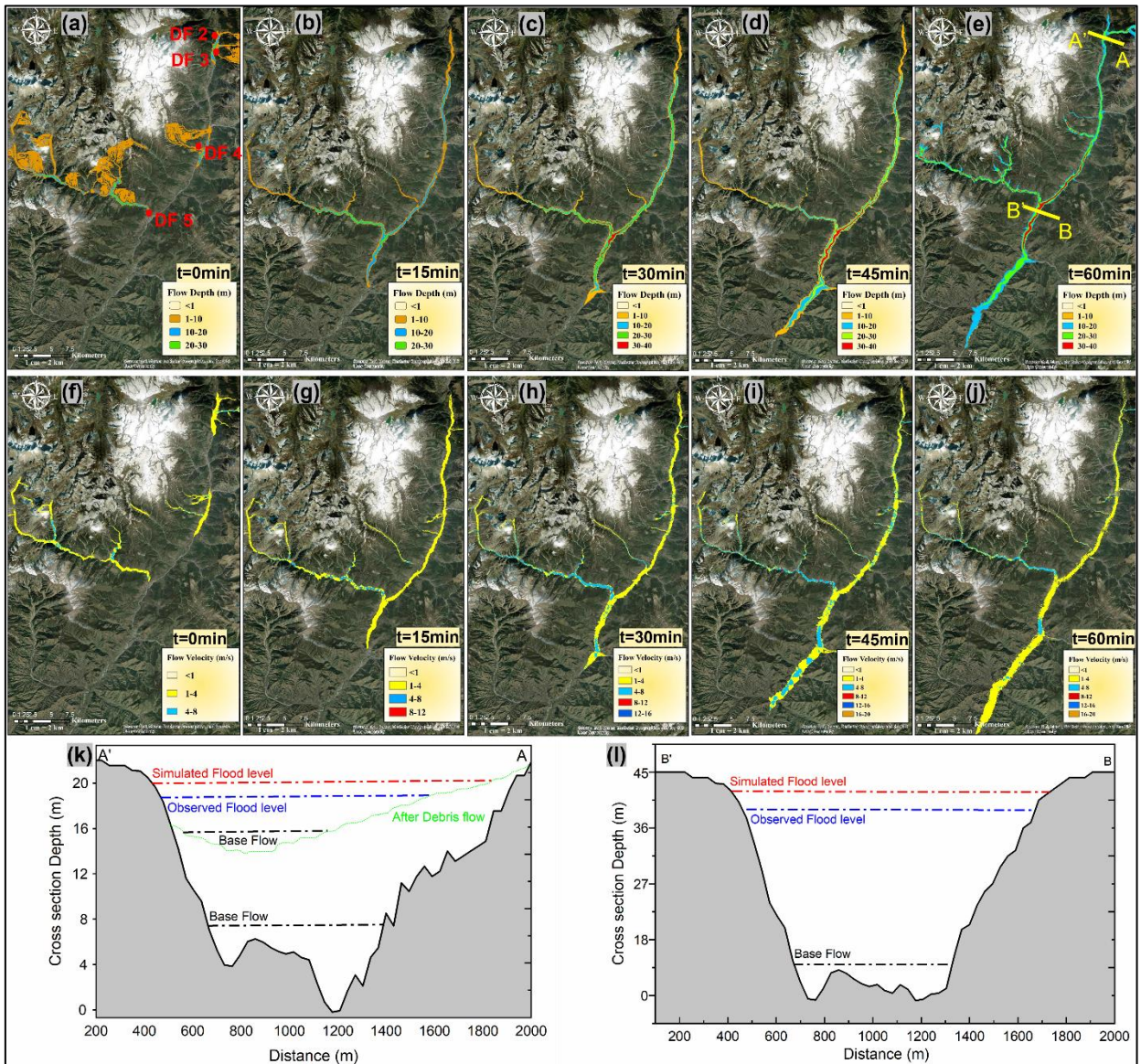


Figure 8. Simulated results of four impactful debris flows affecting the surrounding areas and contributing to the Swat River. Panel (a) shows the main debris flow and its source areas. Panels (b-e) illustrate the initiation and depth of the debris flows, while panels (f-j) showcase the corresponding velocities. Panels (k) and (l) compare the observed and simulated flood levels. Cross-sections depicted in panel (e) (A'A and B'B) are detailed in panels (k) and (l), explaining the observed and simulated flood levels at these cross-sections. The green horizontal dashed line in panel (k) shows the debris dam in the Swat River and the base flow before and after the debris flow. The background image is taken from © Google Earth.

The debris flow depth peaks between 45 minutes and 60 minutes at 36-40 m, and the velocity peaks at 17-18 m/s, reaching its maximum in panels d-e and i-j, respectively. The average peak velocity upon exiting the gullies is 12-15 m/s, and the depth of the massive material reaches 30-36 m. The influence and contribution of debris flow in the Swat River significantly accelerate flood flow when it enters residential areas along the river. The average velocity increases to 15 to 16



m/s, and the depth rises to 20-30 m (Fig. 8d). Panel k presents the cross-section at DF 2 (A'A), where the debris flow blocks the river. Such scenarios always recorded catastrophic downstream (Chen et al., 2024), and the same here. Before the debris flow, the observed depth reached 18 m, and the simulated recording was 20 m. However, after the debris flows, the blockage occurs in a narrow path, holding the storage of water for a long time. These blockages suddenly breached and recorded considerable damages downstream. In Panel l, the cross-sections of DF 5 (B'B) are depicted. Due to its higher drainage area, the magnitude was high, and many sediments migrated downstream. It did not cause blockage, but considerable damages occurred due to the high magnitude along the stream, as presented in Fig. 8. The resulting floods, characterized by high velocity and magnitude, contribute to the destruction and damage of roads, houses, bridges, and farmland.

4.8. Impact and reason for structure damages

The catastrophic geological hazards identified in the preceding section have severely damaged the area's buildings, bridges, and roads. Most of the structural damage was caused by the direct impact of debris in the gullies. Along the River Swat, buildings were affected by flash floods triggered by the rupture of dams located at DF 2 and DF 5. The details of facilities damaged by debris and flash floods are illustrated in Fig. 8a-j. In Gabral, situated upstream of Kalam, 50 residential buildings were completely damaged due to the direct impact of debris (DF 1). Moving to Kalam Bazar, six residential buildings suffered partial damage caused by the flooding in the Swat River, and one commercial building was washed away. At the location of Budai Kamar (DF 2), the impact of debris destroyed 42 residential buildings, while at DF 3, 20 residential buildings were also entirely damaged by the effects of debris. In Bahrain Bazar, approximately 400 commercial buildings and 9 residential buildings were damaged by the flood triggered by the rupture of the debris dam formed at DF 2. Moreover, the damages at Bahrain Bazar were further intensified by the debris at DF 5, which destroyed 45 residential buildings at Daral Stream (DF 5). At Madyan, most buildings were damaged due to the flood in the River Swat except at DF 6 and DF 7 locations. In Madyan, the flood destroyed 37 residential and 12 commercial structures, and the direct impact of debris flow damaged 20 residential buildings." buildings.

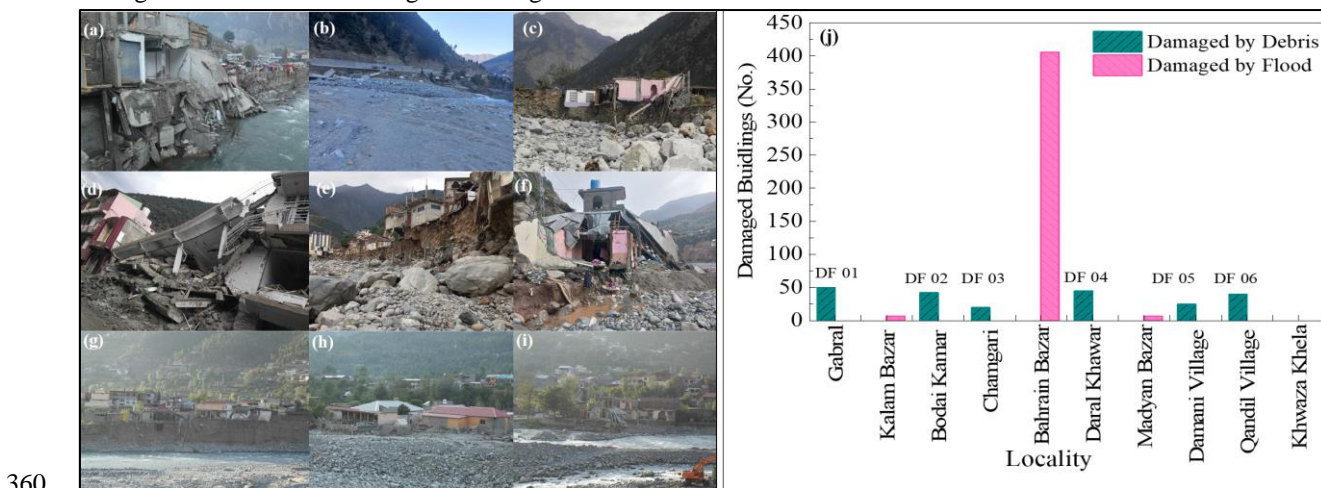
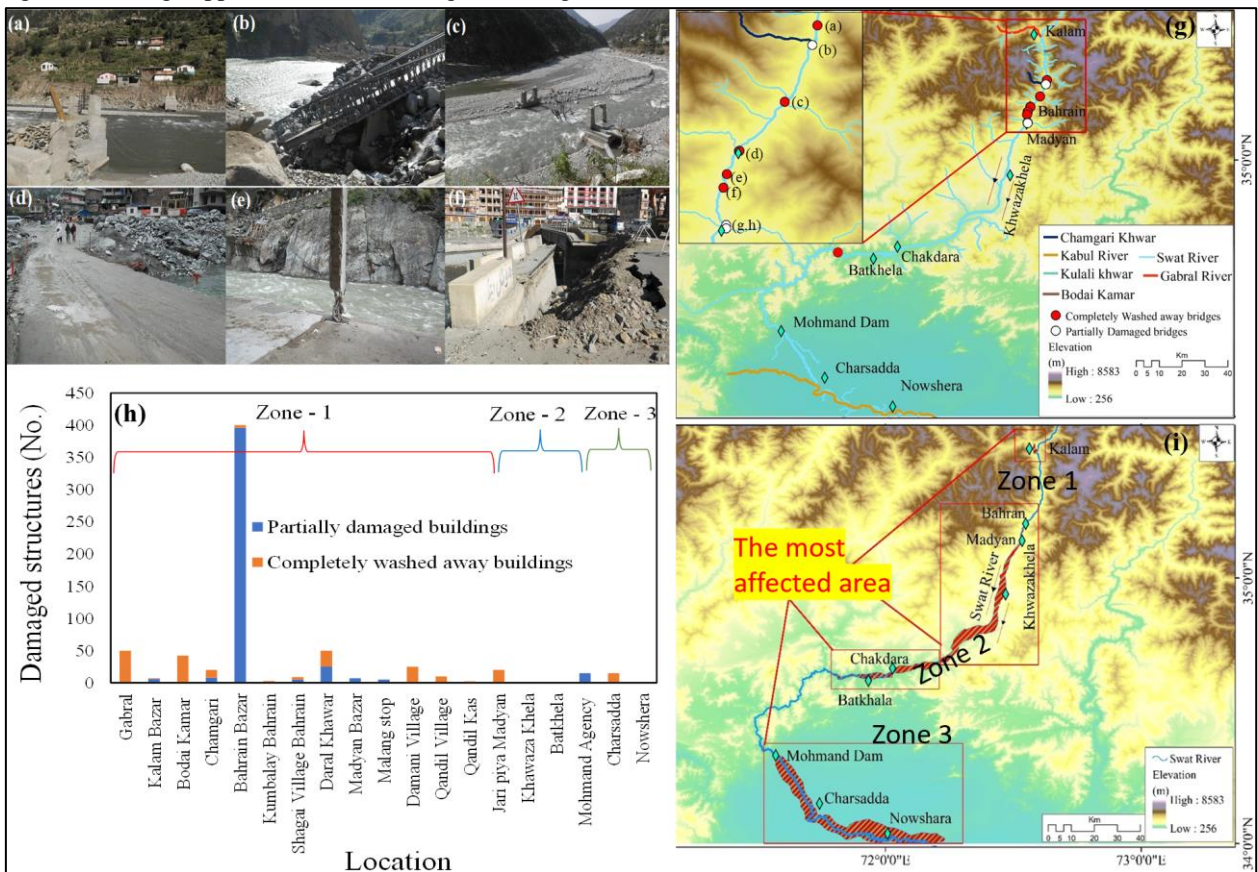


Figure 9. Structural Damages Unveiled: (a) Kalam, (b) Bodai Kamar Khwar (DF 02), (c) Changari Khar (DF 04), (d) Bahrain Bazar, (e) Daral Khwar (DF 05), (f) Near Bahrai Bazar, (g) Bahrain, (h) DF 06, (i) DF 07. Panel (j) provides a numerical breakdown of damages caused by individual debris flows and floods. The background of photos taken during a field visit.

On August 26, 2022, a total of 8 bridges were damaged by the flood along the River Swat. Out of the 8 bridges, 5 were thoroughly washed away. At the same time, 2 were partially damaged (Fig. 9). Most of the bridges collapsed due to



370 elevated flood levels and the accumulation of debris in the River Swat. The Khatak Abad Mankyal bridge, situated upstream
 of Bahrain, experienced a partial collapse of its abutments and thoroughly washed away its wooden deck due to substantial
 debris flow and high-level pressure in the area (Fig. 9a). The direct impact of the debris flow in the gully damaged the
 Chamgari Bridge. The considerable debris (DF 2) blocked the bridge's opening and exerted pressure on the abutment and
 deck. The bridge abutment failed due to overturning, resulting in the bridge's overall failure (Fig. 9b). At the sharp curve of
 the river, the Kedam Bridge, located upstream of Bahrain, was entirely washed away. The bridge's low deck height, the
 elevated flood level, and debris caused the forceful flushing out of the bridge deck (Fig. 9c). Similarly, two bridges at
 Bahrain bazar (junction of River Swat and Daral Khwar (DF 5)) were washed away due to the thrust of flood and debris
 375 (Fig. 9d&e). Two bridges sustained significant damage at Madyan, which is downstream of Bahrain. The destruction
 resulted from the blockage of high-pressure floodwater and debris at the upstream side of the bridges, causing complete
 damage to the bridge approaches and retaining walls (Fig. 9f).



380 **Figure 10.** Unveiling Damaged Bridges along the Swat River: (a) Khatak Abad Mankyal Bridge, (b) Chamgari Bridge, (c)
 Kedam Bridge, (d&e) Bahrain Bazar Bridges, (f) Ayin Village Madyan Bridge, (g&h) Bridges at Madyan Bazar (details
 provided in the supplementary file). Panel (h) illustrates the count of wholly and partially damaged buildings in various
 zones within the most affected areas, as presented in panel (i). The background of photos of panels (a to f) taken during a
 field visit and the SRTM DEM were used for panels (g and i).

385 In addition to residents, commercial properties, and bridges, road damage along the River Swat was also observed and
 reported. The road was mainly damaged at the point of the river bend. The road sections were destroyed due to slope failure
 or retaining wall failure. In Kalam, a road spanning approximately 5 km suffered damage, while in Bahrain, a 4 km road was



affected. Additionally, the road from Bahrain to Khwazakhala experienced damage of 3 km in certain sections. Below is a picture of damaged highways and their location. To better illustrate the extent of damage in regions along the Swat River, we have divided the study area into three zones (refer to Fig. 9(I)): Zone 1, Zone 2, and Zone 3. Zone 1 consists of Gabral, Kalam, Bahrain, and Madyan. Zone 2 includes Khazakhela, Chakdara, Batkhela, and Malakand Agency. Lastly, Zone 3 comprises Mohmand Agency, Charsada, and Nowshera. Zone 1 has faced severe damage to its infrastructure due to hazards and the flooding of the Swat River caused by heavy rainfall. Furthermore, the section of the river in this region is narrow, leading to high flood levels. Zone 2 encountered less damage than Zone 1 due to the broader river section in this region. Additionally, people have become more cautious about building in flood zones after learning from the 2010 flood incident. In Zone 3, the river runs through a gorge in the Malakand Mountains until it reaches Charsada city. Moreover, after the flood in 2010, a flood dam was built in Nowshera, safeguarding the city against flood-related harm.

5. Discussion

The findings of this study align with and build upon the broader body of literature examining the impacts of extreme weather events and geological hazards in the context of global climate change. Previous research has established that climate change exacerbates the frequency and intensity of extreme weather events, leading to increased vulnerability to natural disasters such as debris flows and floods (Masson-Delmotte et al., 2021). This study extends these insights by providing a detailed case study of the 2022 monsoon season in the Swat River basin, offering a comprehensive analysis that incorporates field investigations, remote sensing data, and numerical simulations. Similar to studies by Petley (2012) and Sidle and Ochiai (2006), our research highlights the critical role of land cover changes, particularly deforestation and river encroachments, in increasing the susceptibility of regions to debris flows. As noted in our findings, the transformation of land from grasslands to barren areas reflects global trends where deforestation has been linked to increased runoff and land degradation ((Lal, 2001; Bradshaw et al., 2009). Furthermore, the rapid velocity and significant depth of debris flow observed in our numerical simulations are consistent with the mechanisms described by Hungr et al. (2002) and Choi and Liang (2024), underscoring the importance of topographical and meteorological factors in initiating and propagating debris flows. These high flow velocities are a major factor contributing to river erosion, building demolition, road and bridge damage, and loss of life in the Swat River area. By integrating these elements, our study provides a detailed and nuanced understanding of the interplay between extreme rainfall, deforestation, and topography within the context of the Swat River basin, as elaborated and discussed below.

5.1. The Changes in Current and Historical Trends of Monsoon Rainfall Intensity

During the 2022 monsoon season, which lasted for two months, the country experienced unprecedented rainfall, surpassing all historical records of average rainfall from 1960 to 2021. The 2022 monsoon recorded a 180% increase in rainfall compared to the country's historical average (Qamer et al., 2023). The most intense rainfall event of the season occurred in the Swat River basin between August 25 and August 28, 2022. Particularly on August 26, 2022, heavy rainfall intensity reached an astounding 71.5 mm/day, accompanied by an antecedent rainfall of an average of 40 mm over four days (see Fig. 1b). This extreme precipitation generated significant runoff and catalyzed multiple debris flows along the River Swat.



425 August, typically considered the wettest month in 2022, witnessed an accumulative rainfall reaching an average maximum of 270 mm (Metrological Department of Pakistan). Besides meteorological factors, deforestation emerged as a crucial contributing factor to the high runoff observed during the 2022 monsoon. Evidence of deforestation was prominently depicted in Fig. 3, illustrating a notable expansion of barren land from 15% in 2001 to 24% in 2022. This transformation highlights an alarming increase in land degradation and significant shifts in land utilization (Potić et al., 2022).

430 The encroachment on forested areas has been a continuous trend since 2001. Notably, the affected area served as a tourist attraction and a vital source of income for local communities (Shafiq et al., 2020). The combination of increased rainfall and deforestation has significantly altered the landscape and ecological dynamics of the region (Mehmood et al., 2018; Dogan and Karpuzcu, 2022). Furthermore, deforestation has been linked to reductions in river discharge, highlighting the intricate relationship between forest cover and water resources (Stickler et al., 2013). In summary, the 2022 monsoon season was marked by unprecedented rainfall, particularly in August, with severe consequences, including debris flows. The interplay of meteorological factors and deforestation played a crucial role in exacerbating runoff and land degradation (Austin et al., 2019), emphasizing the need for sustainable land management practices to mitigate future risks.

5.2. The Deforestation Impact on High Runoff and Debris Flow Generation

435 The catastrophic events outlined in this paper serve as compelling evidence that deforestation has significantly impacted the region over the past decade, rendering it highly susceptible to more frequent occurrences of massive debris flow during the rainy season. Consequently, these debris flows transport considerably larger debris from the source area, posing a grave and substantial threat to ongoing restoration and reconstruction endeavors. Based on our investigations, it has been ascertained that the August 26 debris flow was primarily triggered by an exceptionally prolonged rainfall period spanning over four days (Fig. 3) rather than being solely influenced by an unusually high peak rainfall intensity of short duration. Prolonged rainfall can affect slope stability (Volpe et al., 2022). It has the potential to induce a saturated zone, leading to elevated pore water pressures, which, in turn, can contribute to the initiation of a landslide and its subsequent transformation into debris flows (Cojean, 1994; Chen et al., 2006; Farnsworth et al., 2019).

445 Deforestation is pivotal in exacerbating these geological hazards by altering the landscape's natural resilience mechanisms. Landslide deposits resulting from deforestation are often characterized by high permeability, potentially expediting debris flow formation (Rahman et al., 2022). Given that the minimum rainfall intensity and duration required to trigger such events differ across regions, it is crucial to ascertain the prevailing conditions specific to the area under investigation in this paper. By determining these conditions, rainstorm forecasts can be utilized for early warning systems in vulnerable areas, enabling timely responses within a few hours (Campbell et al., 1989; Valente-Neto et al., 2015). The analysis of the collected field data indicates that the characteristics and spatial distribution of rainfall-induced landslides and steep topography played a crucial role in determining the locations of debris flow initiation zones. According to our findings, the runoff in the catchment areas exhibited sufficient force to mobilize a significant quantity of loose debris from the widespread landslides, ultimately transforming them into debris flows. This mechanism has been proposed by Montgomery et al. (2000) and Chen et al. (2006). The numerical simulation analysis has further elucidated that the triggered debris flow had substantial depth and velocity. On average, the velocity increased to 18 m/ sec with an average debris depth of 40 m in 45 min. This accelerated flow significantly amplifies flooding in residential areas along the Swat River, causing substantial destruction to infrastructure and farmland. The present study has shown that rainfall-triggered landslides in different streams along the River Swat provide a tremendous volume of loose landslide debris in the debris flow source area.



5.3. The main reason for damages, losses, and challenges

460 Before this catastrophic event, people in the region were aware of debris flows but did not fully realize their potential for
causing widespread and devastating impacts (Borga, 2012; Guo et al., 2021; Lijuan et al., 2017). The evaluation of debris
flow hazards along River Swat had neglected mainly the interconnected effects of natural disaster chains, such as creating
debris dams, dammed lakes, and floods. Thus, newly constructed infrastructure needed to be prepared and coded for the
sudden and devastating impact of debris flow after a rainstorm of extreme intensity. As a result, the newly built
465 infrastructure was ill-equipped to handle the abrupt and catastrophic effects of debris flow following an extremely intense
rainstorm (Stancanelli and Musumeci, 2018). The event of 26 August 2022 indicates that debris flows are likely to develop
shortly in the regions because of shallow slope failures, altering the landform and simultaneously resulting in disastrous
events (Li et al., 2021). The occurrence on August 26, 2022, suggests that the areas are prone to the future development of
debris flows, mainly due to shallow slope failures. These events can modify the landform and lead to disastrous
470 consequences (Malagó et al., 2018). It is essential to highlight that identifying the areas susceptible to potential inundation
by future debris flows and estimating the flow volume are necessary steps to quantify debris flow hazards effectively. These
measures will facilitate appropriate land use planning to mitigate the risks posed by such events (Rodrigues et al., 2021). The
risk of debris flows has significantly escalated as numerous pre-existing alluvial fans are now being utilized or considered as
resettlement areas in various gullies along the River Swat.

475 Because many pre-existing alluvial fans are being utilized or considered as resettlement areas in the different gullies
along River Swat (Islam et al., 2022a), the risk due to debris flows has dramatically increased. To mitigate debris flows in
the gullies along the River Swat, it is crucial to implement not only engineering measures but also non-engineering
approaches. These non-engineering measures include implementing land use zoning regulations to control and limit the
utilization of hazardous areas. Additionally, relocating people residing in regions prone to debris flows and related flooding
480 to safer locations is essential for effective mitigation.

The catastrophic event discussed in this paper has caused a severe impact on Pakistan's overall financial stability.
Approximately 33 million individuals (roughly equal to 15% of the total population) were impacted. At the same time, the
calamity destroyed 1.5 million residences and inflicted approximately \$2.3 billion in crop damages, with real infrastructural
damage of \$30 billion. Moreover, it caused extensive harm, affecting over 2000 km of roads and severing connectivity to
485 provinces and major urban centers (Acaps, 2022; Liao, 2012). Consequently, inflation in Pakistan has surged to its peak at
approximately 44.5%, signaling an impending and severe food crisis (Banking, 2022). To avoid such consequences in the
future, proper measures should be taken to reduce the impact of climate change, forestation should be encouraged by federal
and local authorities, and construction in flood plans and areas susceptible to debris flows should be discouraged (Pramova
et al., 2012). By prioritizing sustainable land use practices, promoting forest conservation, and implementing adequate
490 disaster risk reduction strategies, Pakistan can enhance its resilience to monsoon-induced geological hazards and mitigate the
socio-economic impacts of such catastrophic events.

5.4. Key Findings and Recommendations

The 2022 monsoon season in the study area brought about a harsh reality check, revealing the interconnected challenges of
extreme rainfall and deforestation. To mitigate future disasters, we must adopt a comprehensive approach and models that
495 can evaluate events in rapid responses (Gorr et al., 2022; Wang et al., 2024; De Brito and Evers, 2016). First, early warning
systems should be fine-tuned to account for local factors, offering timely responses to impending calamities (Nanditha et al.,
2023). Simultaneously, stringent land use planning and zoning regulations must be enforced to limit construction in high-risk
areas, focusing on identifying regions prone to debris flows.



500 Long-term strategies should prioritize reforestation efforts, pivotal in stabilizing slopes, regulating water flow, and
mitigating rainfall-related risks. Lastly, addressing the root causes of extreme weather events is paramount (De Brito and
Evers, 2016). Intensified climate change mitigation, reduced greenhouse gas emissions, and climate-resilient agricultural
practices can contribute to the region's more secure and stable future (Perkins et al., 2012; Nastos and Dalezios, 2016). This
multifaceted approach, informed by the hard-learned lessons of the 2022 monsoon season, is essential to safeguard the
environment and the well-being of the local communities. Furthermore, the lessons gleaned from the 2022 floods emphasize
505 the urgency of adapting to more frequent and severe natural disasters in a warming world, highlighting the necessity for
proactive climate adaptation strategies (Kamal, 2023). The severe impact of floods on public health, particularly the rise in
waterborne diseases like dengue fever, underscores the critical importance of addressing health risks exacerbated by flooding
events (Schmitt et al., 2023).

This study highlights the intricate relationship between deforestation and extreme climate conditions, which
510 significantly alter mountain landscapes and trigger geological hazards, leading to severe impacts on infrastructure, GDP, and
public health. Global deforestation at a rate of 10 million hectares per year and a 7-8% increase in extreme monsoon rainfall
have escalated the frequency of geological hazards. From 1998 to 2017, landslides affected approximately 4.8 million people
and caused over 18,000 fatalities worldwide (WHO). With rising temperatures and climate change expected to worsen these
events, particularly in the Asia-Pacific region—the most disaster-prone area globally—the urgency for effective disaster
515 management strategies is paramount. This study offers a detailed analysis of the 2022 geological hazards caused by rainfall
and deforestation, underscoring the need for reforestation and improved land use planning. By providing empirical evidence
and practical insights, it calls for a redefinition of current strategies, advocating for sustainable practices to mitigate the
impacts of climate change and natural hazards. This reinforces the critical need for holistic and proactive approaches in
disaster management to address the complex challenges posed by these geological hazards

520 6. Conclusion

The 2022 monsoon season unfolded as an unprecedented event, crushing historical records of average rainfall dating back to
1960. Across the country, a notable 7–8% increase in rainfall was observed compared to the historical average. However, the
Swat River basin experienced the season's most intense rainfall, peaking at an astonishing 71.5 mm/day on August 26, 2022,
following an average of 40 mm of precipitation over the preceding four days. This extreme precipitation event catalyzed
525 multiple debris flows along the Swat River, particularly in the Bodai Kamar and Daral Khwar gullies.

The geographical and morphological layout of the drainage area plays a crucial role in determining the spatial
arrangement and commencement of debris flows. Examination reveals that most landslides triggered by rainfall were
concentrated on gradients exceeding 30 degrees, with 83% of these landslides transpiring at slope angles between 40 and 70
degrees. The confluence of meteorological factors and deforestation was pivotal in exacerbating runoff and land degradation
530 during the 2022 monsoon season. The stark transformation of barren land from 15% in 2001 to 24% in 2022 illustrates the
alarming increase in land degradation and shifts in land utilization. This deforestation has altered the rainfall patterns that
trigger slope failures. Consequently, it can be inferred that the key elements contributing to debris flow initiation in this area
are heavy rainfall, steep catchment topography, and a substantial presence of debris. Field investigations further reveal that
the debris supply primarily originates from shallow landslides, channel rill erosion on large landslides, alluvium along the
535 channels, and colluvium and alluvium sourced from the channel banks. The field investigation also revealed that the shallow
landslides within the gullies led to the formation of small debris dams, and their subsequent rupture played a significant role
in intensifying flash flooding and debris flows. Numerical simulations revealed that the debris flows had a significantly high
velocity of 18 m/sec with an average depth of 40 m, reaching this velocity and depth in 45 minutes. The continuous



540 encroachment on forested areas, driven partly by their appeal as tourist attractions and sources of income for local communities, has further exacerbated the landscape's ecological dynamics.

545 The aftermath of the August 26, 2022 events underscores the region's susceptibility to future debris flows, primarily attributed to shallow slope failures. This calls for a holistic approach to debris flow risk management, encompassing stringent regulations on hazardous activities, relocating vulnerable populations, and establishing monitoring and early warning systems. Additionally, addressing the underlying causes of such extreme events, including climate change mitigation and sustainable reforestation efforts, is imperative to secure a more resilient future for the region. This multifaceted strategy, informed by the lessons of the 2022 monsoon season, is crucial for protecting the environment and the well-being of local communities. This paper has pinpointed the most vulnerable regions in Pakistan. The analysis presented here will inspire others to delve deeper into the impact of climate change, specifically focusing on temperature fluctuations, historical rainfall patterns, floods, seismic events, and more.

550 **Authorship Contribution Statement**

NAB and MA: Conceptualization, Methodology, Software, Data curation, and drafting. **PC:** Conceptualization, Supervision, funding acquisition, writing-review and editing, Investigation. **APK, WH, MW, YS, and MR:** Conceptualization, Methodology, Software, **TA, and LW:** Data curation, Investigation. **WH:** Writing-review and editing, Investigation, Formal analysis, Visualization.

555 **Declaration of competing interest**

The authors declare that they have no known competing financial interests or personal relationships that could have appeared to influence the work reported in this paper.

Acknowledgments

560 We thank the Department of Irrigation and Water Resources, NDMA, and PMD for their support in providing the necessary data. Special acknowledgment should be expressed to the China-Pakistan Joint Research Center on Earth Sciences, Islamabad, Pakistan. This study was financially supported by the National Natural Science Foundation of China (Grant no. 42350410445), the Second Tibetan Plateau Scientific Expedition and Research Program (STEP) (No. 2019QZKK0906), and the National Natural Science Foundation of China (Grant no. 4231101214; and 42201086).

565



References

- 570 ACAPS: ACAPS Briefing Note: Pakistan Floods (31 August 2022), 2022.
Alexander, D.: Applied geomorphology and the impact of natural hazards on the built environment, *Natural Hazards*, 4, 57-80, 1991.
- Ali, S., Ali, W., Khan, S., Fawad, M., and Javed, M. W.: Landuse-land cover change assessment in Swat valley, *Journal of Himalayan Earth Sciences*, 45, 23, 2012.
- 575 Atta-ur-Rahman: Disaster risk management: flood perspective, VDM Publishing 2010.
- Austin, K. G., Schwantes, A., Gu, Y., and Kasibhatla, P. S.: What causes deforestation in Indonesia?, *Environ. Res. Lett.*, 14, 024007, 2019.
- Banking, G. C.: Climate-driven floods push Pakistan inflation to 44.5%, 2022.
- Bazai, N. A., Cui, P., Zhou, K. J., Abdul, S., Cui, K. F., Wang, H., Zhang, G. T., and Liu, D. Z.: Application of the soil conservation service model in small and medium basins of the mountainous region of Heilongjiang, China, *Int. J. Environ. Sci. Technol. (Tehran)*, 10.1007/s13762-021-03136-1, 2021.
- 580 Bonnesoeur, V., Locatelli, B., Guariguata, M. R., Ochoa-Tocachi, B. F., Vanacker, V., Mao, Z., Stokes, A., and Mathez-Stiefel, S.-L.: Impacts of forests and forestation on hydrological services in the Andes: A systematic review, *Forest Ecology and Management*, 433, 569-584, 2019.
- 585 Borga, M.: Forecasting, early warning and event management: non-structural protection measures for flash floods and debris flows, in: *Dating Torrential Processes on Fans and Cones: Methods and Their Application for Hazard and Risk Assessment*, Springer, 391-398, 2012.
- Bradshaw, C. J., Sodhi, N. S., and Brook, B. W.: Tropical turmoil: a biodiversity tragedy in progress, *Front. Ecol. Environ.*, 7, 79-87, 2009.
- 590 Bu, C.-f., Wu, S.-f., and Yang, K.-b.: Effects of physical soil crusts on infiltration and splash erosion in three typical Chinese soils, *International Journal of Sediment Research*, 29, 491-501, 2014.
- Campbell, R. H., Fleming, R. W., Prior, D., Nichols, D., Varnes, D. J., Hampton, M. A., Sangrey, D. A., and Brabb, E. E.: *Landslide classification for identification of mud flows and other landslides*, 1989.
- Cepeda, J., Höeg, K., and Nadim, F.: Landslide-triggering rainfall thresholds: a conceptual framework,
- 595 Chen, G., Chong, Y., Meng, X., Yang, Y., Yue, D., Jin, J., Bian, S., Shi, W., and Zhang, Y.: Experimental field study on the formation process of debris flow dam at channel confluence: Implications for early identification of river blockage, *Landslides*, 1-14, 2024.
- Chen, H., Dadson, S., and Chi, Y.-G.: Recent rainfall-induced landslides and debris flow in northern Taiwan, *Geomorphology*, 77, 112-125, 2006.
- 600 Choi, C. E. and Liang, Z.: Segmentation and deep learning to digitalize the kinematics of flow-type landslides, *Acta Geotech.*, 1-20, 2024.
- Cojean, R.: Role of water as triggering factor for landslides and debris flow, *International conference and field workshop on floods*, Trento, Italy,
- Davis, R. S.: Flash flood forecast and detection methods, in: *Severe convective storms*, Springer, 481-525, 2001.
- 605 De Brito, M. M. and Evers, M.: Multi-criteria decision-making for flood risk management: a survey of the current state of the art, *NHESS*, 16, 1019-1033, 2016.
- Dogan, F. N. and Karpuzcu, M. E.: Effect of land use change on hydrology of forested watersheds, *Ecohydrology*, 15, e2367, 2022.



- Farnsworth, A., Lunt, D. J., Robinson, S. A., Valdes, P. J., Roberts, W. H. G., Clift, P. D., Markwick, P. J., Su, T.,
610 Wrobel, N., Bragg, F., Kelland, S.-J., and Pancost, R. D.: Past East Asian Monsoon Evolution Controlled by
Paleogeography, *Not CO₂*, *Sci. Adv.*, 10.1126/sciadv.aax1697, 2019.
- García-Ruiz, J. M., Beguería, S., Alatorre, L. C., and Puigdefábregas, J.: Land cover changes and shallow
landsliding in the flysch sector of the Spanish Pyrenees, *Geomorphology*, 124, 250-259, 2010.
- Georgakakos, K. P. and Hudlow, M. D.: Quantitative precipitation forecast techniques for use in hydrologic
615 forecasting, *Bull. Am. Meteorol. Soc.*, 65, 1186-1200, 1984.
- Gorr, A. N., McGuire, L. A., Youberg, A. M., and Rengers, F. K.: A progressive flow-routing model for rapid
assessment of debris-flow inundation, *Landslides*, 19, 2055-2073, 2022.
- Guo, X., Li, Y., Chen, X., Zhang, J., and Sun, Y.: Variation of debris flow/flood formation conditions at the
watershed scale in the Wenchuan Earthquake area, *Landslides*, 18, 2427-2443, 2021.
- 620 Hungr, O., Evans, S., Bovis, M., and Hutchinson, J.: A review of the classification of landslides of the flow type
(vol 7, pg 225, 2001), *ENVIRONMENTAL & ENGINEERING GEOSCIENCE*, 8, 2002.
- Hürlimann, M., Copons, R., and Altimir, J.: Detailed debris flow hazard assessment in Andorra: a
multidisciplinary approach, *Geomorphology*, 78, 359-372, 2006.
- Hürlimann, M., Guo, Z., Puig-Polo, C., and Medina, V.: Impacts of future climate and land cover changes on
625 landslide susceptibility: Regional scale modelling in the Val d'Aran region (Pyrenees, Spain), *Landslides*, 1-20,
2022.
- Islam, F., Riaz, S., Ghaffar, B., Tariq, A., Shah, S. U., Nawaz, M., Hussain, M. L., Amin, N. U., Li, Q., and Lu, L.:
Landslide susceptibility mapping (LSM) of Swat District, Hindu Kush Himalayan region of Pakistan, using GIS-
based bivariate modeling, *Front. Environ. Sci.*, 10, 1027423, 2022a.
- 630 Islam, F., Riaz, S., Ghaffar, B., Tariq, A., Shah, S. U., Nawaz, M., Hussain, M. L., Amin, N. U., Li, Q., Lu, L., Shah, M.,
and Aslam, M.: Landslide susceptibility mapping (LSM) of Swat District, Hindu Kush Himalayan region of
Pakistan, using GIS-based bivariate modeling, *Frontiers in Environmental Science*, 10,
10.3389/fenvs.2022.1027423, 2022b.
- Julien, P. Y. and Lan, Y.: Rheology of hyperconcentrations, *Journal of Hydraulic Engineering*, 117, 346-353,
635 10.1061/(ASCE)0733-9429(1991)117:3(346), 1991.
- Kamal, A.: Climate, Floods, and Migration in Pakistan, *Int. Migr.*, 10.1111/imig.13170, 2023.
- Kreft, S., Eckstein, D., and Melchior, I.: Global climate risk index 2014, Who suffers most from extreme weather
events, 1, 2013.
- Lal, R.: Soil degradation by erosion, *LDD*, 12, 519-539, 2001.
- 640 Li, M., Tian, S., Huang, C., Wen-qia, W. U., and Xin, S.: Risk Assessment of Highway in the Upper Reaches of
Minjiang River Under the Stress of Debris Flow, *Journal of Geoscience and Environment Protection*,
10.4236/gep.2021.97002, 2021.
- Liao, K. H.: A Theory on Urban Resilience to Floods--a Basis for Alternative Planning Practices, *Ecol. Soc.*,
10.5751/es-05231-170448, 2012.
- 645 Lijuan, W., Chang, M., Dou, X., Ma, G., and Yang, C.: Analysis of River Blocking Induced by a Debris Flow,
Geofluids, 10.1155/2017/1268135, 2017.
- Ma, M., Wang, H., Yang, Y., Zhao, G., Tang, G., Hong, Z., Clark, R. A., Chen, Y., Xu, H., and Hong, Y.: Development
of a new rainfall-triggering index of flash flood warning-case study in Yunnan province, China, *Journal of Flood
Risk Management*, 14, 10.1111/jfr3.12676, 2020.
- 650 Malagó, A., Bouraoui, F., and Roo, A. d.: Diagnosis and Treatment of the SWAT Hydrological Response Using the
Budyko Framework, *Sustainability*, 10.3390/su10051373, 2018.



- 655 Masson-Delmotte, V., Zhai, P., Pirani, S., Connors, C., Péan, S., Berger, N., Caud, Y., Chen, L., Goldfarb, M., and Scheel Monteiro, P. M.: Ipcc, 2021: Summary for policymakers. in: *Climate change 2021: The physical science basis. contribution of working group i to the sixth assessment report of the intergovernmental panel on climate change, 2021.*
- Mehmood, M., Yaseen, M., Ud-Din, I., Badshah, A., and Khan, M.: Causes of deforestation and its geological impacts in Swat District, Khyber Pakhtunkhwa, Pakistan, *Asian Journal of Environment & Ecology*, 5, 1-9, 2018.
- 660 Mehtab, A., Jiang, Y.-J., Su, L.-J., Shamsheer, S., Li, J.-J., and Mahfuzur, R.: Scaling the roots mechanical reinforcement in plantation of *cunninghamia R. Br* in Southwest China, *Forests*, 12, 33, 2020.
- Montgomery, D. R., Schmidt, K. M., Greenberg, H. M., and Dietrich, W. E.: Forest clearing and regional landsliding, *Geology*, 28, 311-314, 2000.
- Nanditha, J., Kushwaha, A. P., Singh, R., Malik, I., Solanki, H., Chuphal, D. S., Dangar, S., Mahto, S. S., Vegad, U., and Mishra, V.: The Pakistan flood of August 2022: Causes and implications, *Earth's Future*, 11, e2022EF003230, 2023.
- 665 Nastos, P. T. and Dalezios, N. R.: Preface: Advances in meteorological hazards and extreme events, *NHESS*, 16, 1259-1268, 2016.
- NWS, I.: *National Weather Service Glossary*, 2009.
- O'Brien, K. L., Sygna, L., Leichenko, R., Adger, W. N., Barnett, J., Mitchell, T., Schipper, E. L. F., Tanner, T., Vogel, C., and Mortreux, C.: *Disaster Risk Reduction, Climate Change Adaptation and Human Security: A Commissioned Report for the Norwegian Ministry of Foreign Affairs by the Global Environmental Change and Human Security (GECHS) Project*, 2008.
- 670 Otto, F. E. L., Zachariah, M., Saeed, F., Siddiqi, A., Kamil, S., Mushtaq, H., Arulalan, T., AchutaRao, K., Chaithra, S. T., Barnes, C., Philip, S., Kew, S., Vautard, R., Koren, G., Pinto, I., Wolski, P., Vahlberg, M., Singh, R., Arrighi, J., van Aalst, M., Thalheimer, L., Raju, E., Li, S., Yang, W., Harrington, L. J., and Clarke, B.: Climate change increased extreme monsoon rainfall, flooding highly vulnerable communities in Pakistan, *Environmental Research: Climate*, 2, 10.1088/2752-5295/acbfd5, 2023.
- Ouyang, C., He, S., and Tang, C.: Numerical analysis of dynamics of debris flow over erodible beds in Wenchuan earthquake-induced area, *Engineering Geology*, 194, 62-72, 10.1016/j.enggeo.2014.07.012, 2015a.
- 680 Ouyang, C., He, S., and Xu, Q.: MacCormack-TVD Finite Difference Solution for Dam Break Hydraulics over Erodible Sediment Beds, *Journal of Hydraulic Engineering*, 141, 10.1061/(asce)hy.1943-7900.0000986, 2015b.
- Ouyang, C., He, S., Xu, Q., Luo, Y., and Zhang, W.: A MacCormack-TVD finite difference method to simulate the mass flow in mountainous terrain with variable computational domain, *Comput Geosci*, 52, 1-10, 2013.
- Ouyang, C., Wang, Z., An, H., Liu, X., and Wang, D.: An example of a hazard and risk assessment for debris flows—A case study of Niwan Gully, Wudu, China, *Engineering Geology*, 263, 10.1016/j.enggeo.2019.105351, 685 2019a.
- Ouyang, C., Zhou, K., Xu, Q., Yin, J., Peng, D., Wang, D., and Li, W.: Dynamic analysis and numerical modeling of the 2015 catastrophic landslide of the construction waste landfill at Guangming, Shenzhen, China, *Landslides*, 14, 705-718, 10.1007/s10346-016-0764-9, 2016.
- 690 Ouyang, C., An, H., Zhou, S., Wang, Z., Su, P., Wang, D., Cheng, D., and She, J.: Insights from the failure and dynamic characteristics of two sequential landslides at Baige village along the Jinsha River, China, *Landslides*, 16, 1397-1414, 10.1007/s10346-019-01177-9, 2019b.
- Perkins, S. E., Alexander, L. V., and Nairn, J.: Increasing Frequency, Intensity and Duration of Observed Global Heatwaves and Warm Spells, *Geophys. Res. Lett.*, 10.1029/2012gl053361, 2012.
- Petley, D.: Global patterns of loss of life from landslides, *Geology*, 40, 927-930, 2012.



- 695 Potić, I., Mihajlović, L. M., Šimunić, V., Ćurčić, N. B., and Milinčić, M.: Deforestation as a cause of increased surface runoff in the catchment: Remote Sensing and Swat Approach—A case study of southern Serbia, *Frontiers in Environmental Science*, 10, 896404, 2022.
- Pramova, E., Locatelli, B., Djoudi, H., and Somorin, O. A.: Forests and Trees for Social Adaptation to Climate Variability and Change, *Wiley Interdisciplinary Reviews Climate Change*, 10.1002/wcc.195, 2012.
- 700 Preti, F., Dani, A., Alliu, E., and Togni, M.: Deforestation and Danger from Surface Landslide, XXXII National Hydraulic Conference and Hydraulic Constructions. Palermo, 14-17,
- Prochaska, A. B., Santi, P. M., Higgins, J. D., and Cannon, S. H.: Debris-flow runout predictions based on the average channel slope (ACS), *Engineering Geology*, 98, 29-40, 2008.
- 705 Qamer, F. M., Abbas, S., Ahmad, B., Hussain, A., Salman, A., Muhammad, S., Nawaz, M., Shrestha, S., Iqbal, B., and Thapa, S.: A framework for multi-sensor satellite data to evaluate crop production losses: the case study of 2022 Pakistan floods, *Scientific Reports*, 13, 4240, 2023.
- Rahman, G., Bacha, A. S., Ul Moazzam, M. F., Rahman, A. U., Mahmood, S., Almohamad, H., Al Dughairi, A. A., Al-Mutiry, M., Alrasheedi, M., and Abdo, H. G.: Assessment of landslide susceptibility, exposure, vulnerability, and risk in shahpur valley, eastern hindu kush, *Frontiers in Earth Science*, 1348, 2022.
- 710 Reichenbach, P., Busca, C., Mondini, A., and Rossi, M.: The influence of land use change on landslide susceptibility zonation: the Briga catchment test site (Messina, Italy), *Environmental management*, 54, 1372-1384, 2014.
- Rickenmann, D., Laigle, D., McArdeell, B. W., and Hübl, J.: Comparison of 2D debris-flow simulation models with field events, *Computational Geosciences*, 10, 241-264, 10.1007/s10596-005-9021-3, 2006.
- 715 Rodrigues, J. A. M., Andrade, A. C. d. O., Viola, M. R., Ferreira, D. D., Mello, C. R. d., and Thebaldi, M. S.: Hydrological Modeling in a Basin of the Brazilian Cerrado Biome, *Ambiente E Agua - An Interdisciplinary Journal of Applied Science*, 10.4136/ambi-agua.2639, 2021.
- Schmitt, R. J. P., Virgüez, E., Ashfaq, S., and Caldeira, K.: Move Up or Move Over: Mapping Opportunities for Climate Adaptation in Pakistan's Indus Plains, *Environ. Res. Lett.*, 10.1088/1748-9326/acfc59, 2023.
- 720 Segoni, S., Piciullo, L., and Gariano, S. L.: Preface: Landslide early warning systems: monitoring systems, rainfall thresholds, warning models, performance evaluation and risk perception, *NHESS*, 18, 3179-3186, 2018.
- Shafiq, M., Nasir, J., Batool, S., Naeem, K., Batool, H., Mehmood, S. A., Shahzad, M., Talib, B., and Arif, H.: Spatiotemporal Analysis of Land Use / Land Cover in Swat, Pakistan Using Supervised Classification in Remote Sensing: 2000 to 2015, *International Journal of Economic and Environmental Geology*, 11, 69-74,
- 725 10.46660/ijeeg.Vol11.Iss2.2020.450, 2020.
- Shah, S. J. H.: Role of Institutions in Combating the Effects of Flood Hazard in Punjab-a Case Study of District Chiniot, 1, 31-41, 10.34154/2020-assj-0202-33-43/eurass, 2020.
- Sidle, R. and Ochiai, H.: Processes, prediction, and land use, *Water resources monograph. American Geophysical Union, Washington*, 525, 2006.
- 730 Sidle, R. C.: A theoretical model of the effects of timber harvesting on slope stability, *Water Resources Research*, 28, 1897-1910, 1992.
- Špitalar, M., Gourley, J. J., Lutoff, C., Kirstetter, P.-E., Brilly, M., and Carr, N.: Analysis of flash flood parameters and human impacts in the US from 2006 to 2012, *JHyd*, 519, 863-870, 2014.
- 735 Stancanelli, L. M. and Musumeci, R. E.: Geometrical Characterization of Sediment Deposits at the Confluence of Mountain Streams, *Water*, 10.3390/w10040401, 2018.



- Stickler, C. M., Coe, M. T., Costa, M. H., Nepstad, D. C., McGrath, D. G., Dias, L. C., Rodrigues, H. O., and Soares-Filho, B. S.: Dependence of hydropower energy generation on forests in the Amazon Basin at local and regional scales, *Proceedings of the National Academy of Sciences*, 110, 9601-9606, 2013.
- 740 Stoffel, M.: Magnitude–frequency relationships of debris flows—A case study based on field surveys and tree-ring records, *Geomorphology*, 116, 67-76, 2010.
- Tang, G., Clark, M. P., Papalexiou, S. M., Ma, Z., and Hong, Y.: Have satellite precipitation products improved over last two decades? A comprehensive comparison of GPM IMERG with nine satellite and reanalysis datasets, *Remote Sens. Environ.*, 240, 111697, 2020.
- Tang, G., Zeng, Z., Ma, M., Liu, R., Wen, Y., and Hong, Y.: Can near-real-time satellite precipitation products
745 capture rainstorms and guide flood warning for the 2016 summer in South China?, *IEEE Geosci. Remote Sens. Lett.*, 14, 1208-1212, 2017.
- Tsukamoto, Y.: Effect of vegetation on debris slide occurrences on steep forested slopes in Japan Islands, *Effect of vegetation on debris slide occurrences on steep forested slopes in Japan Islands.*, 183-191, 1990.
- 750 Valente-Neto, F., Koroiva, N. R., Fonseca-Gessner, A. A., and Roque, F. d. O.: The Effect of Riparian Deforestation on Macroinvertebrates Associated With Submerged Woody Debris, *Aquat. Ecol.*, 10.1007/s10452-015-9510-y, 2015.
- Vanacker, V., Vanderschaeghe, M., Govers, G., Willems, E., Poesen, J., Deckers, J., and De Bievre, B.: Linking hydrological, infinite slope stability and land-use change models through GIS for assessing the impact of deforestation on slope stability in high Andean watersheds, *Geomorphology*, 52, 299-315, 2003.
- 755 Volpe, E., Gariano, S. L., Ardizzone, F., Fiorucci, F., and Salciarini, D.: A Heuristic Method to Evaluate the Effect of Soil Tillage on Slope Stability: A Pilot Case in Central Italy, *Land*, 11, 10.3390/land11060912, 2022.
- Wang, T., Yin, K., Li, Y., Chen, L., Xiao, C., Zhu, H., and van Westen, C.: Physical vulnerability curve construction and quantitative risk assessment of a typhoon-triggered debris flow via numerical simulation: A case study of Zhejiang Province, SE China, *Landslides*, 1-20, 2024.
- 760 Ward, P. J., Blauhut, V., Bloemendaal, N., Daniell, J. E., de Ruiter, M. C., Duncan, M. J., Emberson, R., Jenkins, S. F., Kirschbaum, D., and Kunz, M.: Natural hazard risk assessments at the global scale, *NHESS*, 20, 1069-1096, 2020.
- Ying-Hsin, Wu, Ko-Fei, Liu, Yi-Chin, and Chen: Comparison between FLO-2D and Debris-2D on the application of assessment of granular debris flow hazards with case study, *Journal of Mountain Science*, 10.1007/s11629-013-
765 2511-1, 2013.